Contents lists available at http://www.jmsse.org/

Journal of Materials Science & Surface Engineering

Investigation on Electro-Chemical Behavior of Ti-15V-3Cr-3Al-3Sn in Concentrated H$_2$SO$_4$ and HCl Solutions

Hanuma Reddy Tiyyagura[1], K. Chaitanya Kumar[2], K. Koteshwara Reddy[3], M. K. Mohan[1*]

[1]Department of Metallurgical and Material Engineering, National Institute of Technology, Warangal, Telangana-506004 India.
[2]Corrosion & Fouling Division, Bharat Petroleum Corporate R & D Centre, Greater Noida, Uttar Pradesh – 201 306, India.
[3]Dept. of Energy Science and Technology ,Smart Living Innovation Technology Center, Myongji University 116 Myongji-ro Cheoin-gu, Yongin, Gyeonggi-do 17058, Republic of Korea.

Abstract

Titanium alloys are extensively used in aerospace, biomedical and dental applications. Because the stability and corrosion resistance of titanium is found to be very high. This is due to the spontaneous formation of a passive titanium dioxide film, typically a few nanometer thick, which protects the metal from further oxidation. An investigation was carried out to evaluate the electrochemical corrosion resistance behavior of Ti−15V−3Cr−3Al−3Sn (Ti−15−3) in acidic environments, viz., sulfuric acid (H$_2$SO$_4$) and hydrochloric acid (HCl) at different concentrations. Electrochemical impedance (EIS) and potentiodynamic polarization studies were conducted to evaluate the corrosion resistance of the alloy. Both Nyquist and Bode plots were recorded in EIS studies. Bode plots exhibit a broad phase maxima at lower concentrations and the two-time constants at the higher concentration in both the environments. This infers the passivation of the oxide layer in lower concentrations and passivation and dissolution of the oxide film at higher concentrations. The potentiodynamic polarization measurements indicate the active dissolution of native oxide film present on the Ti−15−3 alloy surface at higher concentrations, which is inferred by the presence of active−passive regions in anodic curves in both the environments. The results obtained from both electrochemical impedance and potentiodynamic polarization studies were good agreement with each other. All these studies inferred that there is an adverse effect of sulphate (SO$_4^{2−}$) ions than Cl$^−$ on Ti−15V−3Cr−3Al−3Sn alloy.

Introduction

Titanium and its alloys are promising materials for applications ranging from structural to biomedical implants and aerospace industry because these alloys posses excellent mechanical properties like low density and high tensile and good corrosion resistance[1–6]. Titanium has a strong chemical affinity towards oxygen and hydrogen. It forms a tight film of oxide on the freshly prepared surface like aluminum at room temperature. The oxide film grows with time and makes titanium passive. This nature accounts for excellent corrosion resistance of titanium in oxidizing acid and aqueous salt solutions. Hydride layer formation in cathodic potentials also provides passivity, but its stability is over a short range, at little nobler potentials its existence is debatable[7].

The titanium alloys are classified into α, α+β, meta−stable β, and stable β alloys, based on the phases present [8]. The α−alloys are used for the applications requiring higher corrosion resistance viz., paper and pulp industries. The other grades are used in aerospace and naval applications. In the past few decades, β−alloys emerge as versatile alloys being used for a variety of applications especially aerospace and medical implants[9–11]. β−alloys offer advantages of higher tensile and fatigue strength, ability to heat treat to greater section thicknesses to high strength and easier fabrication into some semi−products[11]. Keeping in view of the stringent requirements for these applications, over the decades, many titanium alloys have been developed [12-13]. Ti−15V−3Cr−3Al−3Sn alloy, which is also referred as Ti−15−3 is

meta−stable β titanium alloy meeting the requirements like high strength along with excellent corrosion resistance properties for fastener material[14,15]. The main strengthening mechanism of this alloy is due to the precipitation of uniformly dispersed fine α phase in the β matrix. In the present study, an investigation has been carried out on the corrosion resistance performance of Ti−15V−3Cr−3Al−3Sn alloy in different acidic solutions (H$_2$SO$_4$ and HCl) at different concentrations. Electrochemical studies viz., electrochemical impedance and potentiodynamic polarization studies were employed to evaluate the corrosion resistance performance. Microstructural studies were also carried out.

Experimental

Materials

Ti−15V−3Cr−3Al−3Sn was supplied by GE WICK (China) through Kalva Engineers Pvt. Limited, Hyderabad. The alloy was procured in sheet form and annealed condition as per the specifications ASTM B265.The chemical composition is given in Table 1. All the chemicals used are of Analar grade. All the specimens were machined and prepared as per ASTM G1 specifications. The specimens of dimension 4x1x0.2 cm were cut from the alloy sheet and polished sequentially using grade 120, 320, 400, 600, 800, 1000 and 1200 emery papers. Finally, the specimens were polished with diamond paste.   After the pre−treatment, the specimens showed a uniform and grease free oxide free surface, thus highly susceptible to corrosion and these were used immediately in corrosion studies. The samples were

Corresponding author. Tel.+91- 870-2462510
E-mail address: mkmohan@nitw.ac.in

etched with Kroll's reagent (6 ml HNO₃, 2 ml HF, and 92 ml distilled water) for 30 seconds. The specimens were exposed to different concentrations of H_2SO_4 (0.5, 1.5, 2.5, 3.5 and 4.5M) and HCl (1.0, 3.0, 5.0, 7.0, and 9.0M) solutions.

Table 1: Composition of Ti-15-3

Alloy	Ti	V	Cr	Sn	Al	Fe	C	N	H	O
Ti-15-3	Remaining	3.0	3.0	3.1	3.0	0.18	0.008	0.027	0.003	0.009

Electrochemical studies

ZAHNER iM6e Electrochemical Workstation (Germany) was used for all the electrochemical experiments with a three-electrode cell assembly. Ti−15V−3Cr−3Al−3Sn as working electrode with an exposed area of 1cm^2, Ag/AgCl/1.0M KCl as a reference electrode and platinum as a counter electrode. Electrochemical impedance measurements were carried out at open circuit potential (OCP) in the frequency range from 10 mHz to 60 kHz with an amplitude of 10 mV. Potentiodynamic polarization experiments were performed within the potential range of −750mV to +250mV vs. Ag/AgCl/ 1.0 M KCl with a scan rate of 2mVs^{-1}.

Results and Discussion

Electrochemical impedance studies

The Electrochemical impedance spectroscopy is a powerful technique for studying spontaneous passivation of metals in the electrolytes. Prior to each experiment the specimen was immersed in the electrolyte for a period of 180 minutes in order to achieve a stabilized open circuit potential. The EIS results are presented in the form of Nyquist and Bode plots.
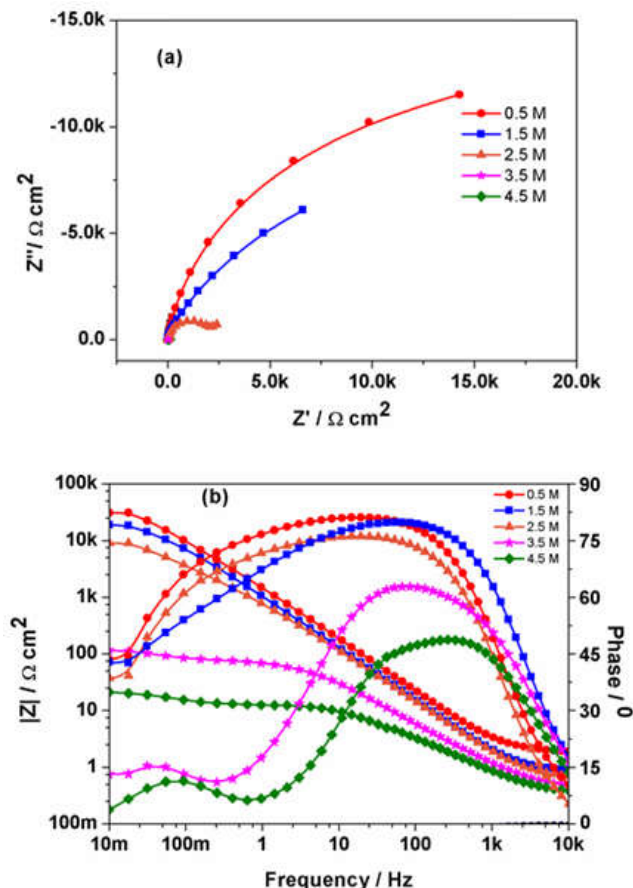
The Nyquist and Bode plots of Ti−15V−3Cr−3Al−3Sn alloy in different concentrations of H_2SO_4 are presented in figures 1a and b respectively. The Nyquist plot showed a semi−circle, which exhibits the capacitive nature of the alloy in H_2SO_4. The diameter of the semi−circle decreases with increase in concentration indicating the decrease in charge transfer resistance (R_{ct}) values w1ith concentration due to the active dissolution of the passive film, which is dominant in the presence of SO_4^{2-} ions. The Bode plots have some distinct advantages over the Nyquist plots as the frequency appears as one of the axis, so it is easy to understand how impedance depends on frequency. The Bode plots show lower impedance at higher concentrate which corresponds to the solution resistance. The Bode plots in H_2SO_4 at different concentrations show two distinctive capacitive behaviors (Figure 1b). The Bode plot also shows the broad phase maxima at lower concentrations indicating the formation of thicker oxide films while the narrow phase maxima is due to thinning of the oxide film[11]. The overlapping time constant separates at higher concentration (3.5M), which may be due to the dissolution and re−passivation of the oxide film. The impedance data was simulated to the appropriate equivalent circuit for the two-time constants by using the equivalent circuit model [16]shown in Figure 2 .
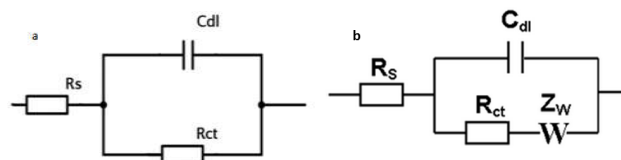

Figure 2: Schematic equivalent circuit diagrams

The electrode is covered with a passive layer, and it is depicted in RC model (Figure 2a), where the resistance is parallel to the capacitance. For the two-time constants impedance response, (Figure 2b) the equivalent model consisting of two circuits in series, i.e. R_1C_1 and R_2C_2, where C_1 represents the capacitance of outer layer and C_2 is the contribution of the capacitance of the inner layer [19] . The impedance parameters obtained from these studies are tabulated in Table 2. The R_{ct} value is decreased from 28.66 to 0.075 kΩ cm^2 with an increase in concentration of H_2SO_4 from 0.5 to 2.5 M. The R_{ct} value again slightly increases at 3.5 M concentration and decreased at 4.5M concentration. Because, at 3.5 M concentration of H_2SO_4, there is both dissolution and repassivation of oxide film occur. The double layer capacitance values (C_{dl}) values are increased with increase in concentration. The Nyquist and Bode plots of Ti−15V−3Cr−3Al−3Sn alloy in different concentrations of HCl are presented in figures 3a and b respectively. The impedance parameters are shown in Table 3.
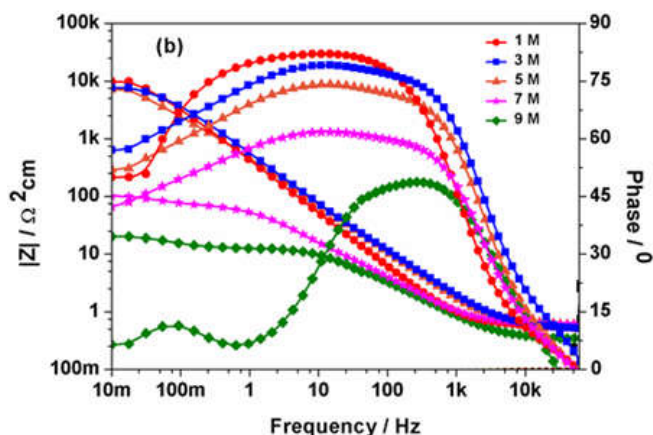

Figure1: (a) Nyquist and (b) Bode plot for Ti-15-3 in H_2SO_4
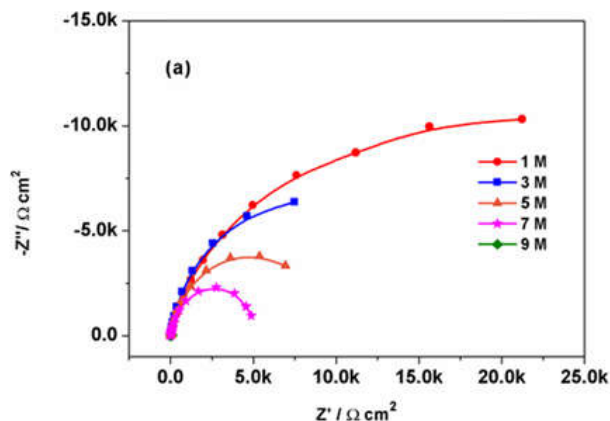
Figure 3: (a) Nyquist and (b) Bode plot for Ti-15-3 in HCl

Table 2: I_{corr} and E_{corr} value of Ti-15-3 in H_2SO_4 at different concentration

Environment	$I_{cor}(\mu A)$	E_{cor} (mV)	Corrosion rate (mpy)	R_p
0.5M H_2SO_4	2.89	-171.9	1.3	28.66
1M H_2SO_4	8.17	-283.9	1.4	15.33
1.5M H_2SO_4	32.8	-360.1	14.7	2.094
2.5M H_2SO_4	123	-362.7	55.0	2.043
3.5M H_2SO_4	135	-370.3	60.3	0.754
4.5M H_2SO_4	250	-372.3	111.7	0.188

Table3: I_{corr} and E_{corr} value of Ti-15-3 in HCl at different concentration

Environment	$I_{cor}(\mu A)$	E_{cor} (mV)	Corrosion rate (mpy)	R_p
1M HCl	1.67	-48.91	0.7	15.57
2M HCl	6.27	-272.8	2.8	11.21
3M HCl	13.7	-280.8	6.1	2.184
5M HCl	125	-288.3	15.2	0.074
7M HCl	34.1	-321.8	55.9	0.0969
9M HCl	50	-353.7	67	0.1356

The diameter of the semi−circle in Nyquist plots decrease with increase in the concentration of HCl indicating the decrease in charge transfer resistance (Rct) values. The broad phase−maxima in Bode plots is also observed in the HCl solution. The presence of the two-time constants is also observed. The R_{ct} values are found to be higher than that of in H_2SO_4 environment, which indicates more corrosive nature of SO_4^{2-} ions. The absolute impedance values were also observed to be higher for HCl solutions than H_2SO_4 solutions at lower frequencies in both acidic solutions. This infers that the SO_4^{2-} ions attack the passive oxide film more vigorously than Cl⁻ ions, indicating the more corrosive nature of SO_4^{2-} ions.

Potentiodynamic polarization studies

The potentiodynamic polarization curves of Ti−15V−3Cr−3Al−3Sn alloy at different concentrations of H_2SO_4 are presented in Figure 4. A fresh solution was prepared for carrying out each experiment to maintain the same ion concentration. Tafel extrapolation method was used for calculating the corrosion potential, corrosion current density, and polarization resistance. The corrosion parameters obtained from these studies were given in Table 4. The corrosion potential (E_{corr}) values are shifted towards more negative potentials. At ≥3.5 M concentration of HCl, anodic peaks exhibit an active−passive transition in between −150 mV to +200 mV. It infers the presence of both dissolution and re−passivation of the oxide film on the alloy surface, which is in good agreement with the result observation seen in impedance studies.
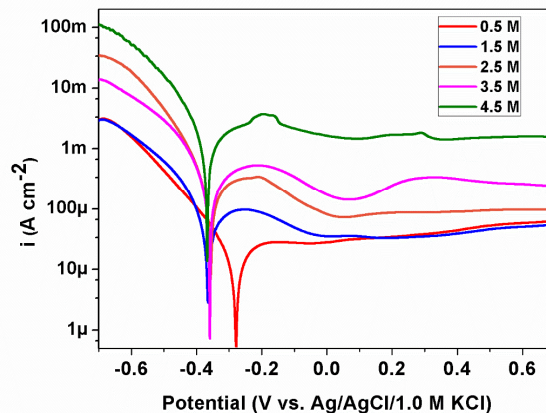

Figure 4: The potentiodynamic polarization curves for Ti-15-3 in H_2SO_4

Table 4: Impedance parameters of Ti-15-3 in H_2SO_4 at different concentration

Environment	Rct(KΩ)	Zw (DW)	Cdl (uF)	Rs (mΩ)
0.5M H_2SO_4	28.66	0.7078	57.78	1819
1M H_2SO_4	15.33	0.3483	85.83	828.4
1.5M H_2SO_4	2.094	3.10	91.81	626.4
2.5M H_2SO_4	0.075	13.87	169.9	424.2
3.5M H_2SO_4	2.043	176.5	112.1	442.8
4.5M H_2SO_4	0.013	1.229	256	347.6

The corrosion current density is significantly increased with increase in the concentration of H_2SO_4. It infers the adverse affect of SO_4^{2-} ions on the alloy. The corrosion rate was calculated. A valence number of 3 was used for calculating the corrosion rates [17]. The potentiodynamic polarization curves of Ti−15V−3Cr−3Al−3Sn alloy at different concentrations of HCl are presented in Figure 5. The corrosion parameters obtained from these studies were given in Table 5. The E_{corr} values are shifted towards more negative potentials. At ≥3.5 M concentration of HCl, anodic peaks exhibit an active−passive transition in between +100 mV to +200 mV. It infers the presence of both dissolution and re−passivation of the oxide film on the alloy surface. For both the media, the i_{corr} value increases with the increase in concentration. The primary passivation potential also became more negative. The corrosion rates are higher in H_2SO_4 when compared with HCl which indicates that more of SO_4^{2-} ions are more corrosive in nature than the Cl⁻ ions. This result is in agreement with the corrosion behavior of pure titanium and Ti−6Al−4V alloy in the same acidic environment[18].
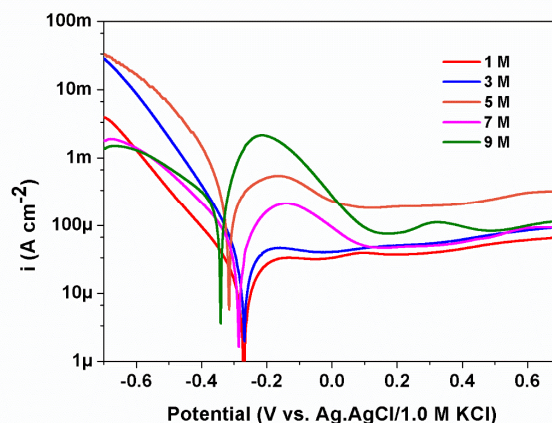

Figure 5: The potentiodynamic polarization curves for Ti-15-3 in HCl

Table 5: Impedance parameters of Ti-15-3 in HCl different concentration

Environment	Rct(KΩ)	Zw (DW)	Cdl (uF)	Rs (mΩ)
1M HCl	15.57	0.3032	34.03	1169
2M HCl	2.184	0.3239	111.8	607.9
3M HCl	11.21	0.1102	212.5	560.7
5M HCl	0.074	12.86	234	585.6
7M HCl	9.699	61.19	96.1	521
9M HCl	5.355	3.086	95.93	501.9

Conclusions

The Ti−5−3 alloy is corroded more in H_2SO_4 acidic environment than HCl environment. Bode plots exhibit two-time constants at the higher concentration in both the environments. This infers the passivation and dissolution of the oxide film at higher concentrations. The potentiodynamic polarization measurements active−passive regions are present in anodic curves in both the environments, which indicates the active dissolution of native oxide film present on the Ti−15−3 alloy surface at higher concentrations.

Acknowledgement

References

1. C. Cui, B. Hu, L. Zhao, S. Liu, Titanium alloy production technology, market prospects and industry development, Materials & Design. 32 (2011) 1684–1691. doi:10.1016/j.matdes.2010.09.011.
2. J. Szewczenko, J. Marciniak, W. Kajzer, A. Kajzer, Evaluation of corrosion resistance of titanium alloys used for medical implants, Archives of Metallurgy and Materials. 61 (2016) 695–699. doi:10.1515/amm-2016-0118.
3. C. Veiga, J. Davim, A. Loureiro, Properties and Applications of Titanium Alloys: a Brief Review, Rev. Adv. Mater. Sci. 32 (2012) 133–148.
4. K. Nageswara Rao, U. V Gururaja, Manufacture of titanium and titanium alloys at Midhani: An overview, Transactions of the Indian Institute of Metals. 61 (2008) 349–354. doi:10.1007/s12666-008-0066-6.
5. R.R. Boyer, An overview on the use of titanium in the aerospace industry, Materials Science and Engineering: A. 213 (1996) 103–114. doi:10.1016/0921-5093(96)10233-1.
6. M. Niinomi, Biologically and Mechanically Biocompatible Titanium Alloys, MATERIALS TRANSACTIONS. 49 (2008) 2170–2178. doi:10.2320/matertrans.L-MRA2008828.
7. N.T. Thomas, K. Nobe, The Electrochemical Behavior of Titanium: Effect of pH and Chloride Ions, Journal of The Electrochemical Society. 116 (1969) 1748–1751. doi:10.1149/1.2411696.
8. J. Donachie, J. M, Titanium – A Technical Guide, ASM International 2nd Edition. 55 (2000) 1023–1026. doi:10.1016/j.scriptamat.2006.08.010.
9. K.V. Sudhakar, K. Konen, K. Floreen, Beta-titanium biomedical alloy: effect of thermal processing on mechanical properties, Archives of Metallurgy and Materials. 57 (2012). doi:10.2478/v10172-012-0082-8.
10. R.R. Boyer, Aerospace applications of beta titanium alloys, JOM. 46 (1994) 20–23. doi:10.1007/BF03220743.
11. S.L. Nyakana, J.C. Fanning, R.R. Boyer, Quick reference guide for β titanium alloys in the 00s, Journal of Materials Engineering and Performance. 14 (2005) 799–811. doi:10.1361/105994905X75646.
12. K. Balachandar, V. Subramanya Sarma, B. Pant, G. Phanikumar, Microstructure and Mechanical Properties of Gas-Tungsten-Arc–Welded Ti-15-3 Beta Titanium Alloy, Metallurgical and Materials Transactions A. 40 (2009) 2685–2693. doi:10.1007/s11661-009-9952-8.
13. G. Rao, M. Rao, B. Rao, P. Sagar, ELECTROCHEMICAL CHARACTERIZATION OF BIOMEDICAL TITANIUM ALLOY Ti-35Nb-7Zr-5Ta, Technicaljournalsonline.Com. (n.d.). http://www.technicaljournalsonline.com/ijeat/VOL III/IJAET VOL III ISSUE I JANUARY MARCH 2012/47 IJAET Vol III Issue I 2012.pdf.
14. R.W. Schutz, Environmental behavior of beta titanium alloys, JOM. 46 (1994) 24–29. doi:10.1007/BF03220744.
15. R. Sarkar, P. Ghosal, T.K. Nandy, K.K. Ray, Tensile and fracture behavior of boron and carbon modified Ti-15-3 alloys in aged conditions, Materials Science and Engineering: A. 656 (2016) 223–233. doi:10.1016/j.msea.2016.01.038.
16. I. Chimica-fisica, P. Milano, P. Leonardo, G. Taccani, B. Vicentini, G. Dallaspezia, Electrochemical Behavior of Titanium and Some Titanium Alloys under Tensile Stress in Boiling Sulfuric Acid and Acidic Chloride Solutions, 1 (n.d.) 4–9.
17. S.D. Cramer, B.S. Covino, ASM Handbook Vol. 13a: Corrosion - Fundamentals, Testing, and Protection, Asm. 13 (2003) 1135. doi:10.1002/jbm.b.31896.
18. A.S. Mogoda, Y.H. Ahmad, W.A. Badawy, Corrosion inhibition of Ti-6Al-4V alloy in sulfuric and hydrochloric acid solutions using inorganic passivators, Materials and Corrosion. 55 (2004) 449–456. doi:10.1002/maco.200303751.